ON-CHIP LIQUID-LIQUID EXTRACTION AND SEPARATION USING DIGITAL MICROFLUIDICS

by

PRAVEEN KUNCHALA

Presented to the Faculty of the Graduate School of

The University of Texas at Arlington in Partial Fulfillment

of the Requirements

for the Degree of

MASTER OF SCIENCE IN MECHANICAL ENGINEERING

THE UNIVERSITY OF TEXAS AT ARLINGTON

December 2009

ACKNOWLEDGEMENTS

I would like to thank my advisor Dr. Hyejin Moon and the University of Texas at Arlington for giving me this opportunity to work in IMNF lab and support. I would like to acknowledge the help I received from Yasith Nanayakkara and Dr. Daniel W. Amstrong's biochemistry lab for the timely supply of Ionic liquids. I sincerely thank my co-workers Nitin, Shreyas, Subin and Jagath for their support in my research.

I would like to thank my parents for their constant and continued love and support for which I will be always grateful and my friends for helping me in all possible ways.

November 24, 2009

ABSTRACT

ON-CHIP LIQUID-LIQUID EXTRACTION AND SEPARATION USING DIGITAL MICROFLUIDICS

PRAVEEN KUNCHALA, M.S.

The University of Texas at Arlington, 2009

Supervising Professor: HYEJIN MOON

In this thesis, on-chip liquid-liquid microextraction and separation using electrowetting on dielectric (EWOD) digital microfluidics was demonstrated by considering room temperature ionic liquid (RTIL) and DI water as two liquid phases, which form immiscible interface with each other. Room temperature ionic liquids (RTILs) have been actively investigated as replacements for the organic solvents and various "task-specific" ionic liquids (TSIL) are being developed which exhibit many attractive properties such as selectivity to specific biomolecules. Liquid-liquid extraction and separation using EWOD digital microfluidic device with model extraction experiments have been demonstrated, one was extraction of organic dye from RTIL (1-butyl-3-methylimidazolium bis(trifluoromethylsulfonyl)imide, [bmim][NTf_2]) into DI water. Second one was extraction of iodine (I_2) from water into [bmim][NTf2]. This demonstration is the first step towards micro total analysis system (μTAS).

An on chip pH dependent partitioning in RTIL's using EWOD operation was performed to demonstrate that pH value of the aqueous solution effect the extraction process. This experiment demonstrates that on chip pH titration and extraction is possible which can lead to High-throughput screening (HTS) synthesis of RTIL's and HTS of protein extraction.

TABLE OF CONTENTS

LIST OF ILLUSTRATIONS

Figure Page

LIST OF TABLES

CHAPTER 1

INTRODUCTION

1.1 Microfluidics

Microfluidics deals with the behavior, precise control and manipulation of fluids that are geometrically constrained to a small, typically sub-millimeter, scale. It is a multidisciplinary field interfaces engineering, physics, chemistry, micro-technology and biology, with practical applications to the design of systems in which such small volumes of fluids will be used. The advantages in using microfluidic systems include fast reaction time(~ms-s), low power consumption, handling of very small sample volumes (nl, pl), high sensitivity, mass production of data, and low cost.

In Microfluidics the Reynolds number is very low and is dominated by viscous force.

$$Re = \frac{\rho \ell \mathcal{V}}{\mu} = \frac{inertial\ force}{viscous\ force}$$

Where $\mathcal{V}$ is mean fluidic velocity, ℓ is characteristic length, ρ is density of fluid, and μ is the dynamic viscosity of the fluid [1]. Low Reynolds number results in laminar flow which will be a challenging task at micro scale.

Advances in Microfluidics technology are revolutionizing molecular biology procedures for enzymatic analysis (e.g., glucose and lactate assays), DNA analysis (e.g., polymerase chain reaction and high-throughput sequencing), and proteomics. The basic idea of Microfluidics biochips is to integrate assay operations such as detection, sample pre-treatment and sample preparation on one chip[2], [3]. An emerging application area for biochips is clinical pathology, especially the immediate point-of-care diagnosis of diseases. In addition, Microfluidics-based devices, capable of continuous sampling and real-time testing of air/water samples for

biochemical toxins and other dangerous pathogens, can serve as an always-on "bio-smoke alarm" for early warning.

Continuous-flow microfluidics through micro channels is one of the early microfluidics systems. Actuation of liquid flow is implemented either by external pressure sources or external mechanical pumps. Figure 1.1 shows an example of continuous flow microfluidics through microfabricated channels.

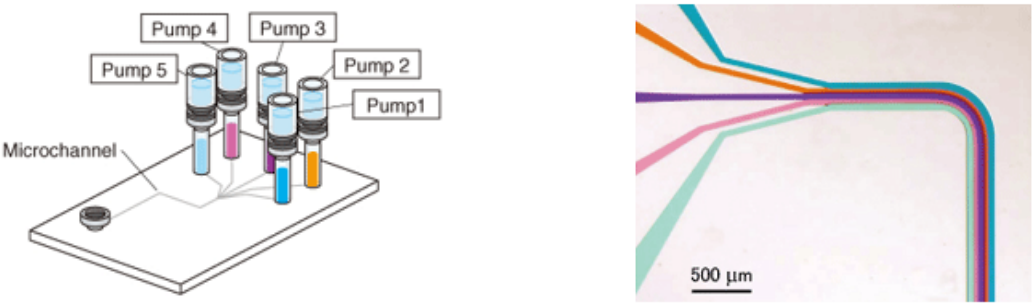

Figure 1.1 Layered laminar flow with 5 externally operated pumps. [4]

Typically micropumps are required for channel-based microfluidic systems. Micropumps control fluid behavior in small channels, taking advantage of the physical properties of the fluid, its contents and channels. A pneumatically driven micropump made of polyimide diaphragm with titanium wire heater is shown in fig 1.2.

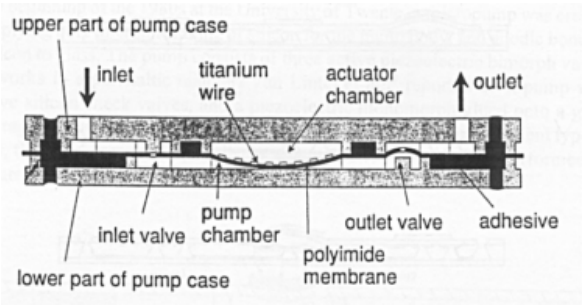

Figure1.2 Micropump fabricated by plastic molding with a polyimide membrane and Ti wire heater. [5]

Microvalves are also needed to control continuous flow in microchannels. Microvalves are generally actuated by reciprocal motion of membrane, which can be induced by various ways, such as temperature change, piezoelectric motion and shape memory alloys motion.

Figure 1.3 shows a schematic cross sectional view of microvalve where the microvalve actuation is dependent on TiNi shape memory film which is thermally actuated.

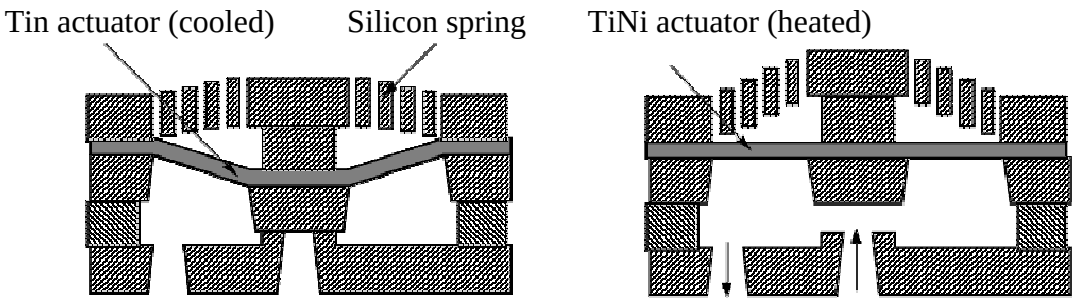

Figure 1.3 Schematic cross section of a microvalve fabricated by bulk micromachining and wafer bonding. The TiNi shape memory film is thermally actuated to open and close the microvalve .[6]

1.2 Digital Microfluidics

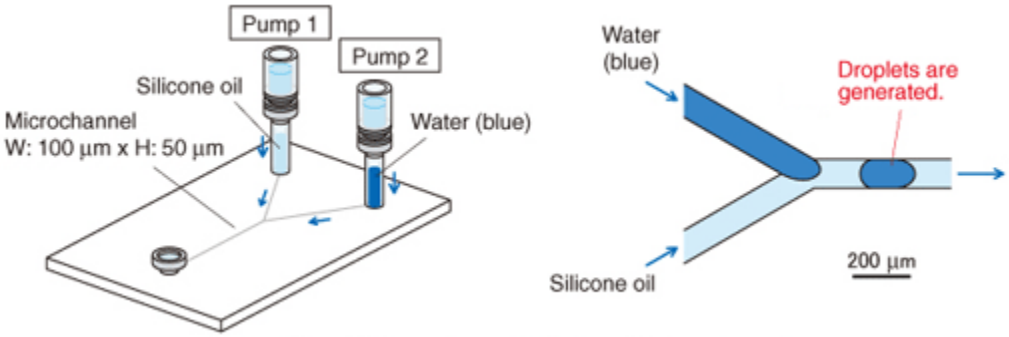

Figure 1.4 Droplets formation with Y-shaped microchannel. [7]

Digital Microfluidics system (DMFS) is based on micromanipulation of discrete droplets. In continuous-flow DMF actuation of liquid flow through micro channels is implemented either by external pressure sources or external mechanical pumps. [8] Figure 1.4 shows an example of continuous flow DMF through microfabricated channels.

Microvalves are another class of DMF where fluid flow in micro channels is generally controlled by reciprocal motion of the membrane. An example of microvalve DMFS is shown in figure 1.5

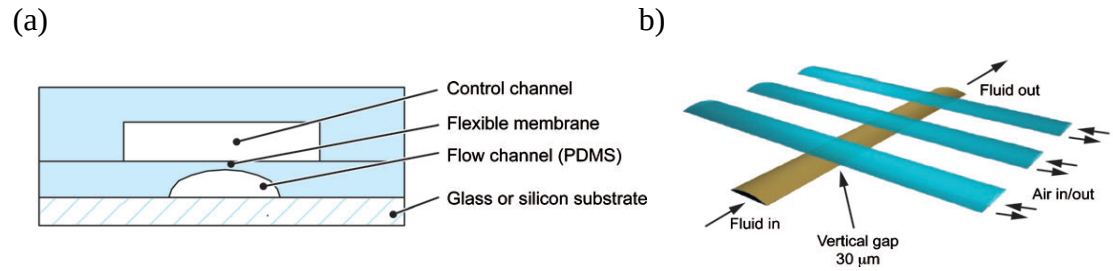

Figure 1.5 Example of a micro-valve (a) a two-layer polydimethylsiloxane (PDMS) push-down Microfluidics valve. An elastomeric membrane is formed where the flow channel is positioned orthogonal to the control channel directly above. Fluid flow is out of the page. (b) Schematic of a linear peristaltic pump using three membrane valves in a series. [9]

Electrowetting has recently been used successfully as one of the several techniques used to actuate microdroplets in a digital microfluidic device. In many of these applications electowetting allows large numbers of droplets to be independently manipulated under direct electrical control without the use of pumps, valves or even fixed channels. This method offers advantages over conventional continuous-flow microfluidic chips, by way of significantly reduced sample size, improving processing of biochemical assays, as well as allowing reconfigurability and scalability of architecture. A DMFS typically consists of a planar array of cells with electrodes that control individual droplets of chemicals; the chemical analysis is performed by moving, mixing, and splitting droplets.

1.3 Electrowetting on Dielectric (EWOD)

When an external electric potential is applied between a liquid and solid or between two immiscible liquids, the charges and dipoles redistribute, modifying the surface energy at the interface. Specifically, the presence of a net electric charge at an interface lowers the surface tension, because repulsion between like charges decreases the work done in expanding the surface area. The mathematical relationship between the applied electric potential (V) and the

resulting surface tension (γ) can be derived by thermodynamic analysis of the interface. The result is expressed in Lippmann's Eq. (1) [10]

$$\gamma=\gamma_o-\frac{1}{2}cV^2 \quad (1)$$

Where γ_o is the surface tension of the solid-liquid interface at the potential zero charge (i.e., no charge at the surface of the solid), and c is the capacitance per unit area, assuming the charge layer can be modeled as a symmetric Helmholtz capacitor.

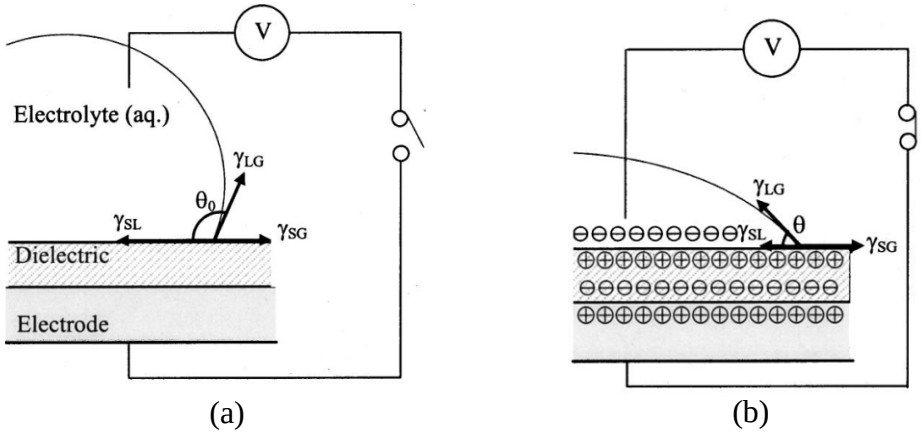

Figure 1.6 Principle of EWOD. (a) With no external voltage applied, there is little or no charge accumulation at the interface. (b) With an external voltage applied, charge accumulates at the interfaces, γ_{SL} and the contact angle θ decreases. [11]

When a dielectric layer inserted between the electrode and the liquid, it can emulate the electric double layer (EDL) in conventional electrowetting. Illustrated in figure 1.4, this is called ''electrowetting on dielectric'' (EWOD). EWOD should be considered as an electrowetting phenomenon for certain material configurations. The ideal dielectric blocks electron transfer, while sustaining the high electric field at the interface that results in charge redistribution when a potential is applied. By using a hydrophobic dielectric, the large initial contact angle provides room for a large $\Delta\theta$ upon electrowetting.[11]

Lippmann's Eq. (1) can be expressed in terms of the contact angle θ by incorporating Young's Eq. (2). The resulting Eq. (3) is called the Lippmann–Young equation.

$$\gamma_{SL} = \gamma_{SG} - \gamma_{LG}\cos\theta \tag{2}$$

$$\cos\theta = \cos\theta_o + \frac{1}{\gamma_{LG}}\frac{1}{2}cV^2 \tag{3}$$

Here, θ_o is the contact angle when the electric field across interfacial layer is zero. γ_{SL} is the solid-liquid surface tension, γ_{LG} is the liquid-gas surface tension, and γ_{SG} is the solid-gas surface tension. Note that γ_{LG} and γ_{SG} are assumed to be constant, independent of applied potential. The contact angle in Eq. (3) is a function of applied voltage between the liquid and electrode. [11]

When a hydrophobic liquid segment is sandwiched between two flat surfaces the segment will be in equilibrium state by balancing the pressure inside the segment and outside the segment. This pressure difference ΔP is expressed by Eq. (4), called Young-Laplace equation.

$$\Delta P = P_v - P_l = \gamma\left(\frac{1}{R_1} + \frac{1}{R_2}\right) \propto \frac{\gamma\cos\theta}{d} \tag{4}$$

Where P_v and P_l are pressure outside the liquid and pressure inside the liquid. γ is surface tension of liquid. R_1 is the circular radius of the drop parallel to surface. R_2 is radius of the liquid segment exposed to air. θ is the contact angle of the liquid. "*d*" is the distance between two flat plates.

When two electrodes are placed side by side and actuated alternatively, contact angle at the actuated electrode changes because of EWOD property. As the equilibrium of the liquid segment is disturbed due to the change in pressure difference the segment shifts towards the actuated electrode to attain equilibrium thus the entire liquid segment moves to the actuated electrode as shown in figure 1.5. The pressure difference ΔP inside the moving droplet is expressed by Eq. (5). Where θ_{tL1}, θ_{bL1}, θ_{tR1}, and θ_{bR1} are contact angles at top left, bottom left, top

right and bottom right surfaces respectively."r_{L1}" and "r_{R1}" are left and right radius of the liquid segment respectively.

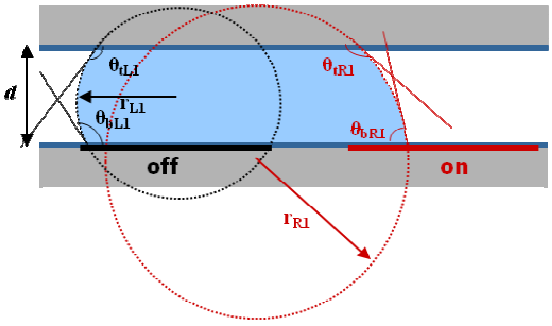

Figure 1.7 Movement of liquid segment by EWOD.

$$\Delta P = \Delta P_L - \Delta P_R = \gamma_{LV}\left(\frac{1}{r_L} - \frac{1}{r_R}\right)$$
$$= \gamma_{LV}\left(\frac{\cos\theta_{bL} + \cos\theta_{tL}}{d} - \frac{\cos\theta_{bR} + \cos\theta_{tR}}{d}\right) \quad (5)$$
$$> 0$$

EWOD digital microfluidics is an efficient platform to process droplet based analytical processes. Nanoliter (nL) or smaller volume of aqueous liquid droplets can be generated and transported on a chip by EWOD process. In addition to the high surface to volume ratio, high chemical potential can be expected in droplet based extraction when the droplets are in motion. [11]-[14]

1.4 Thesis outline

This Thesis reports liquid-liquid microextraction and separation on-chip, using EWOD digital microfluidics by considering two model extraction systems. One is extraction of organic dye from Room temperature Ionic liquid (RTIL) [bmim][NTf2] into DI water and the other is extraction of iodine (I_2) from water into RTIL ([bmim][NTf2]). An on chip pH dependent partitioning in RTILs using EWOD operation was performed to demonstrate that pH value of the aqueous solution effect the extraction process. Importance of RTILs, their flexibility, and applications of task-specific Ionic Liquids (ILs) are demonstrated in this report.

CHAPTER 2

EXPERIMENT

2.1 MEMS Fabrication

Micro-electromechanical system (MEMS) technology can be used to produce complex structures, devices and systems on a microscopic scale (1µm - 100µm). The main advantage of MEMS and devices is that they are smaller, lighter, faster, and usually more precise than their macroscopic counterparts. The development of MEMS devices requires appropriate fabrication technologies which usually involves a structured sequence of operations that enable features such as precise dimensional control, design flexibility, interfacing with control systems, repeatability and reliability. [15]

2.1.1. Photolithography

Photolithography is a process used in microfabrication to selectively remove thin films or bulk of substrate. It uses UV light to transfer a geometric pattern from a photo mask to a chemical photoresist. Photolithography and pattern transfer involves a set of process steps summarized in fig. 2.1. As an example, consider a thin metal layer deposited on a substrate (A) is coated with a photoresist (PR) (~1µm thickness) (B). After exposure (C), the wafer is rinsed in a developing solution which removes the exposed areas of photoresist in case of positive photoresist, and removes unexposed areas of photoresist in case of negative photoresist and leaves a pattern of bare and photoresist-coated metal layer on the substrate surface (D). The photoresist pattern is a positive image of the photomask pattern in case of positive photoresist, and is a negative image in case of negative photoresist. After development, in most common scenario the substrate is placed in a specific metal etching chemical which etches the metal layer and does not affect the phororesist or metal layer underlying it (E). Once the exposed

metal layer has been etched away, the remaining photoresist can be stripped off using liquid strippers involving organic solvent strippers and alkaline strippers (with or without oxidants). [16]

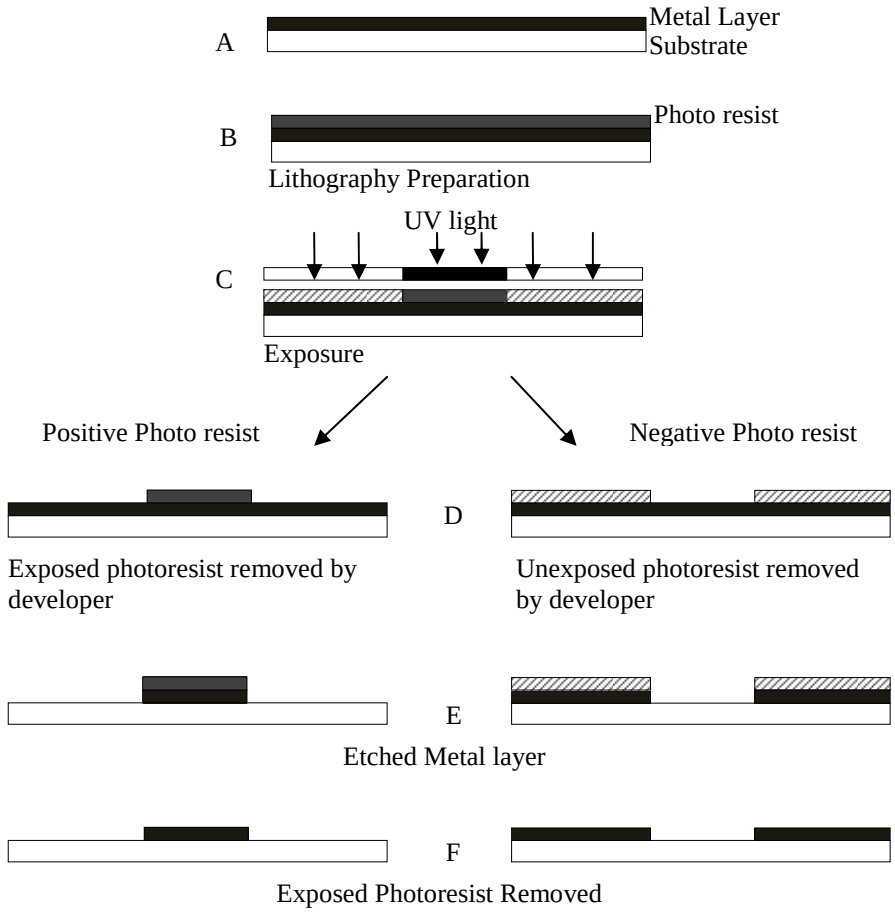

Figure 2.1 Basic lithography and pattern transfer

2.1.2. Spin coating

A common step before spin coating is cleaning the wafer and dehydrating. Spin coating is the first step in the lithography process, a thin layer of a photoresist sensitive to ultraviolet radiation, is being deposited on the wafer surface by spin coating. The photoresist is dispensed onto the wafer lying on a vacuum chuck which holds wafer in place. The wafer is then spun at high speed, between 1500 to 8000 rotations per minute (rpm), depending on the viscosity and required film thickness, to make a uniform film. At such high speeds, centrifugal force causes

the solution to flow to the edges, where it builds up until expelled when surface tension is exceeded. The polymer layer thickness, T, is a function of spin speed, solution concentration, and molecular weight. The empirical expression for T is given by. [1]

$$T = \frac{KC^{\beta}\eta^{\gamma}}{\omega^{\alpha}}$$

Where "K" is overall calibration constant, "C" is polymer concentration in g/100ml solution, "η" is intrinsic viscosity of the polymer, and "ω" is the rotations per minute (rpm) of the vacuum chuck.

2.1.3. Thin-film Process

Thin film deposition process is one of the most important processes in the MEMS fabrication. Generally the Thin films in MEMS systems have a thickness between few nanometes to about 100 micrometers. MEMS deposition technology can be classified in to two group's deposition by chemical reaction and deposition by Physical reaction.

Deposition by chemical reaction covers chemical vapor deposition (CVD), electrodeposition, epitaxy, and thermal oxidation. These processes exploit the creation of solid materials directly from chemical reactions in and/or liquid composition or with the substrate material. The solid material is usually not the only product formed by the reaction. Byproducts can include gases, liquids and even other solids.

Deposition by Physical reaction covers, physical vapor deposition (PVD), thermal evaporation, sputtering, molecular beam epitaxy, laser sputter deposition or ablation deposition, ion plating, cluster beam technology. In all these processes the material deposited is physically moved on to the substrates. In other words there is no chemical reaction which forms the material on the substrate. [2], [3]

2.1.4. Plasma-Enhanced Chemical Vapor Deposition (PECVD)

PECVD is a process used to deposit thin films from a gas state (vapor) to a solid state on a substrate. Chemical reactions are involved in the process, which occur after creation of

plasma from the reacting gases. The plasma is generally created by RF (AC) frequency or DC discharge between two electrodes, the space between which is filled with the reacting gases. Adequate substrate temperature control ensures uniformity of deposition. Wafers are placed on the ground electrode where they are subjected to a less-energetic bombardment than wafers placed on the powered electrode. In most PECVD systems, the reactor configuration is in such a way that the potential of both the powered and the ground electrode, relative to plasma becomes equal. Compared to sputter deposition, PECVD offers several advantages. The lower power densities, higher pressure, and somewhat higher substrate temperatures (>200^{o}C) all lead to less-severe radiation damage than sputter deposition. In addition, selective activation of reactants is possible without damaging the surface of the substrate. PECVD deposition results in good adhesion, low pinhole density, good step coverage, adequate electrical properties, and compatibility with fine line-width pattern transfer process have led to wide use of PECVD in very large scale integration (VLSI). PECVD enables dielectric films such as oxides, nitrides, and oxynitrides to be deposited on small feature sizes and line widths at low temperatures, and on devices unable to withstand the high temperatures of a thermally activated reaction. Another application is the deposition of amorphous-silicon thin films, as used in flat-panel displays, eyeglasses, and photovoltaic panels. The most significant application is probably the deposition of SiO_2 or Si_3N_4 over metal lines. [16]

Figure 2.2 TRION ORION II PECVD/LPCVD System, NANOFAB, UTA. [17]

2.1.5. Etching

Etching can be described as pattern transfer by chemical/physical removal of a material from a substrate- often in a pattern defined by protective mask layer such as resist or an oxide. In general, there are two classes of etching processes: Wet etching and dry etching

In wet etching, features are sculpted in the bulk of materials such as silicon, quartz, Sic, GaAs, InP, and Ge by orientation-independent (isotropic) or orientation-dependent (anisotropic) wet etchants. Some single crystal materials, such as silicon, exhibit anisotropic etching in certain chemicals. Anisotropic etching results in different etch rates in different directions in the material. The classic example of this is the <111> crystal plane sidewalls that appear when etching a hole in a <100> silicon wafer in a chemical such as potassium hydroxide (KOH). The result is a pyramid shaped hole instead of the smoother hole with rounded sidewalls that forms from isotropic etchants. The principle of anisotropic and isotropic wet etching is illustrated in the figure 2.3.

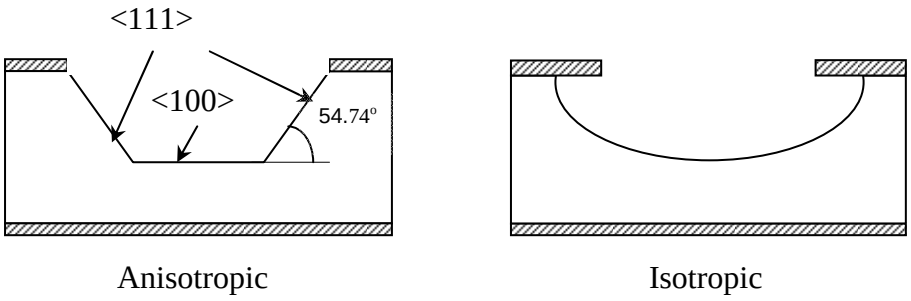

Figure 2.3 Difference between anisotropic and isotropic wet etching. [18]

Dry etching covers many methods by which a solid surface is etched. Methods of dry etching include: gas or vapor phase etching, physical etching, ion bombardment, chemical etching, or by combined physical and chemical mechanisms. The dry etching technology can

split in three separate classes called reactive ion etching (RIE), sputter etching or Ion etching, and vapor phase etching.

In RIE, the substrate is placed inside a reactor in which several gases are introduced. Plasma is created in the gas mixture using an RF power source, which breaks the gas molecules into ions. The ions are accelerated towards, and react at, the surface of the material being etched, forming another gaseous material. This is known as the chemical part of reactive ion etching. There is also a physical part which is similar in nature to the sputtering deposition process. If the ions have enough energy, they can knock atoms out of the material to be etched without a chemical reaction. It is very complex to develop dry etch processes that balance chemical and physical etching, since there are many parameters to adjust. By changing the balance it is possible to influence the anisotropy of the etching, since the chemical part is isotropic and the physical part highly anisotropic and the combination can form sidewalls that have shapes from rounded to vertical.

A special subclass of RIE with which one can fabricate at high-aspect-ratio micromolds is deep RIE (DRIE). In this process, etch depths of hundreds of microns can be achieved with almost vertical sidewalls. The primary technology is based on the "Bosch process", where two different gas compositions are alternated in the reactor. The first gas composition creates a polymer on the surface of the substrate, and the second gas composition etches the substrate. The polymer is immediately sputtered away by the physical part of the etching, but only on the horizontal surfaces and not the sidewalls. Since the polymer only dissolves very slowly in the chemical part of the etching, it builds up on the sidewalls and protects them from etching. As a result, etching aspect ratios of 50 to 1 can be achieved. The process can easily be used to etch completely through a silicon substrate, and etch rates are 3-4 times higher than wet etching.

Sputter etching is essentially RIE without reactive ions. The systems used are very similar in principle to sputtering deposition systems. The big difference is that substrate is now subjected to the ion bombardment instead of the material target used in sputter deposition.

Vapor phase etching is another dry etching method, which can be done with simpler equipment than what RIE requires. In this process the wafer to be etched is placed inside a chamber, in which one or more gases are introduced. The material to be etched is dissolved at the surface in a chemical reaction with the gas molecules. The two most common vapor phase etching technologies are silicon dioxide etching using hydrogen fluoride (HF) and silicon etching using xenon diflouride (XeF2), both of which are isotropic in nature. Usually, care must be taken in the design of a vapor phase process to not have bi-products form in the chemical reaction that condense on the surface and interfere with the etching process.[18]

2.2 Device Fabrication

2.2.1. Mask design

L-Edit software was used to design the mask. The mask was designed in such a way that working electrodes or actuation electrodes where actual EWOD takes place were connected to the contact pads which can be used to provide potential. It has 5 x 5 and 6 x 6 array of electrodes with 4 reservoirs at the corners, as presented in figure 2.4. Figure 2.5 (a) shows individual design of 5 x 5 array chip and figure 2.5 (b) shows the individual design of 6x6 array chip. The reservoir electrodes act as the reservoir for liquids and the rest of actuation electrodes facilitate droplets generation, mixing of the droplets, and separation. The reservoir electrodes are 2mm x 2mm, and all actuation electrodes were 1mm x 1mm in size. All the electrodes were connected to the contact pads with 100 µm strip. The inner actuation electrodes in the circuit were connected to the 100µm strip with a small 10µm strip which runs between the actuation electrodes as shown in figure 2.6.

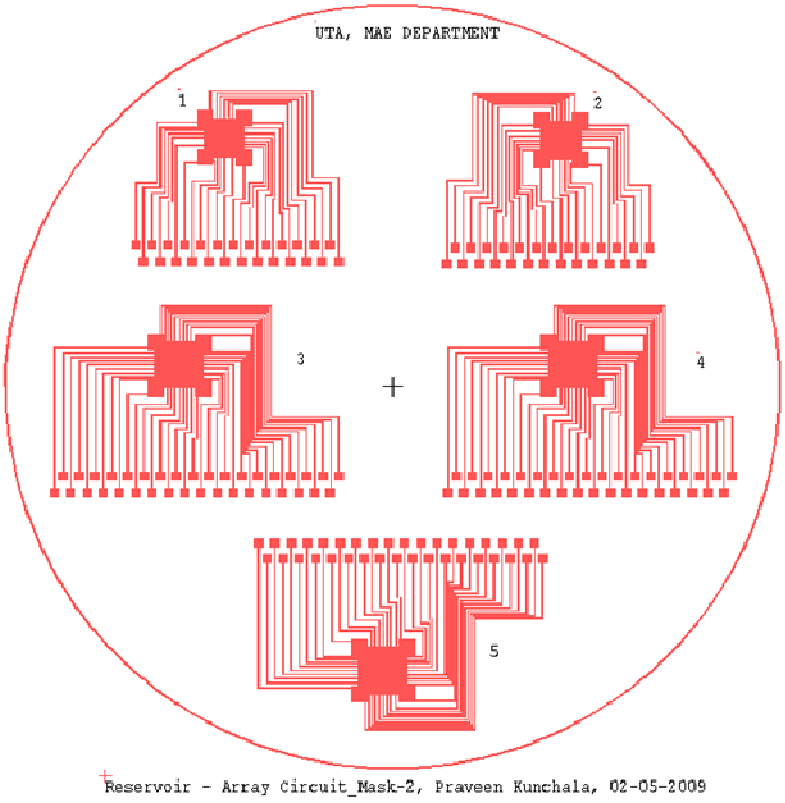

Figure 2.4 Mask design with two 5 x 5 array and 3 6 x 6 array chips.

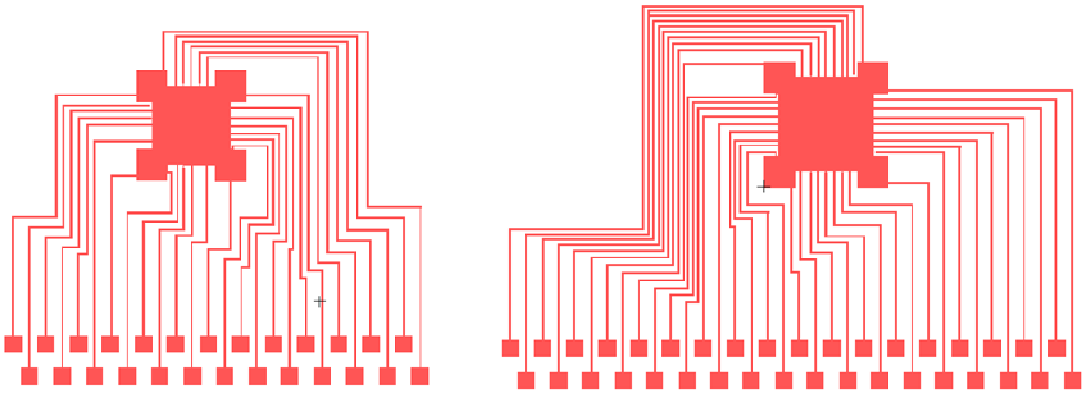

Figure 2.5 Individual chip designs (a) 5 x 5 array chip, (b) 6 x 6 array chip. [19]

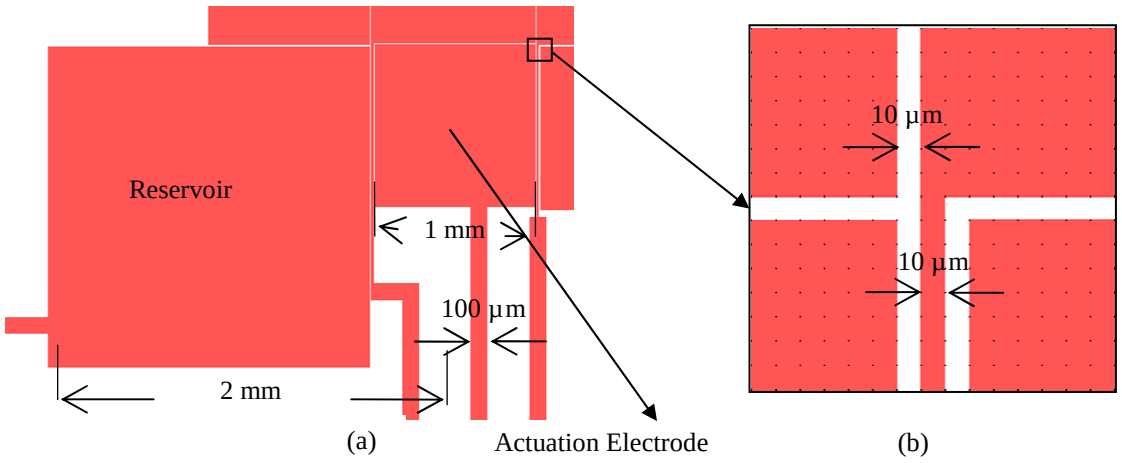

Figure 2.6 Dimensions of the working area on chip (a) Reservoir electrode and Actuation electrode, (b) Magnified view of the selected region in Fig 2.5 (a).

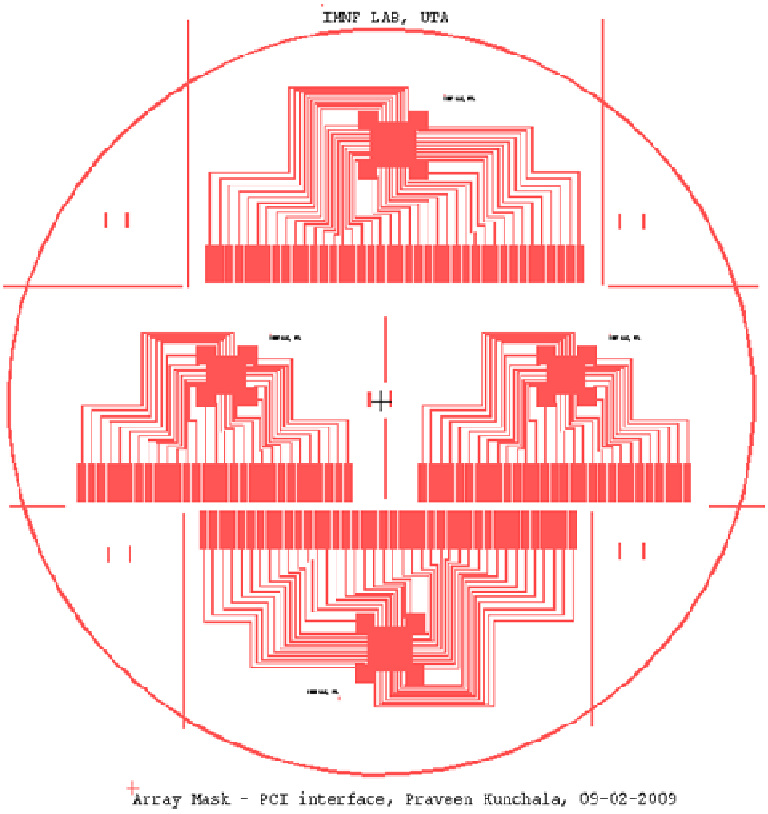

Figure 2.7 PCI-interface Array design.

Initial mask design was modified for further improvements as shown in figure 2.7. Figure 2.8 shows the PCI-interfaced 5 x 5 and 6 x 6 array chips design. Contact pads was redesigned in such a way that the chip can be inserted in to PCI slot just like a PCB board as shown in Figure 2.9. The PCI slot is connected to the Data Acquisition board which is operated through Labview. The reservoir electrode was redesigned by aligning two triangles along their hypotenuse. Actuating both triangles at the same time will give the same effect as a square electrode, and by actuating them individually will benefit the drop by keeping it in touch with actuation electrode, which facilitates in generating more number of droplets when compared to a square electrode.

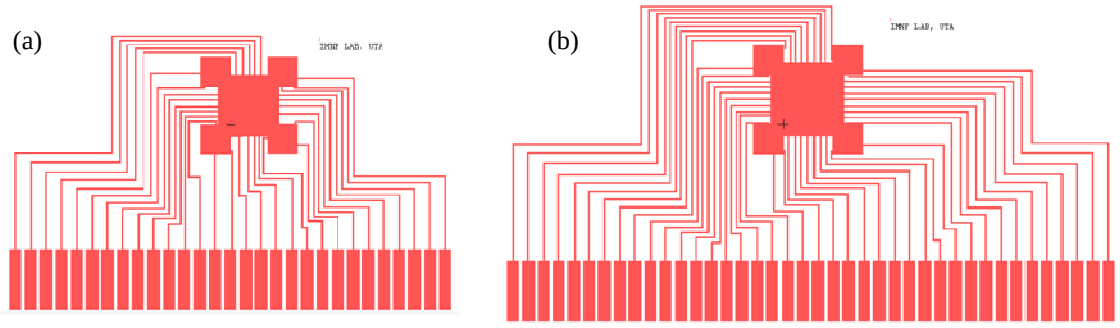

Figure 2.8 Individual PCI-interface chip designs (a) 5 x 5 array chip with PCI-interface, (b) 6 x 6 arrays chip with PCI-interface. [19]

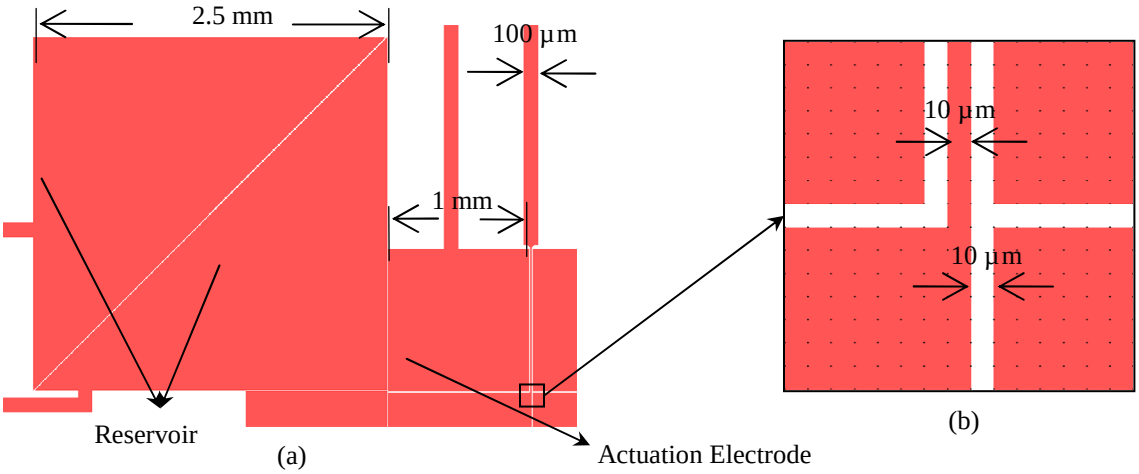

Figure 2.9 Dimensions of the working area on chip in PCI-interface chip design (a) Modified Reservoir electrode,(b) Magnified view of the selected region in (a).

2.2.2. Fabrication process

Digital microfluidic EWOD devices were fabricated at UTA Nanofabrication facility. An Indium tin oxide (ITO) deposited glass wafer was used for subsequent process of Lithography. After lithography, the ITO pattern was etched and then the wafer was diced to individual chips. SiO_2 was used as Dielectric layer in the beginning, and moved on to SU-8 5 as a dielectric layer. SU-8 5 dielectric layer process saves time in the fabrication as we don't need to use PECVD equipment and no pin holes were observed in the dielectric layer, which gives good EWOD movement.

In the fabrication process of EWOD device the first step is to clean ITO wafer and ITO cover slide in 5:1(H_2SO_4 : H_2O_2) Piranha solution for 15 min and dehydrate at 150 ^oC for 10 min. Spin coat wafer with HMDS primer(Microposit Primer) at 4000 rpm for 30 s (ramp rate 900 rpm/s) and then soft-bake it at 150 ^oC for 90 s. Spin coat Shipley 1813 photoresist (PR) (PR) at 4000 rpm for 30 s (ramp rate 900 rpm/s) to form 1.3 μm and soft-bake at 115 ^oC for 1min. Expose the PR coated wafer to UV light using OAI Aligner (I-Line 365 nm) to an expose dosage of 140 mJ/cm^2 for 7 s and then bake at 110 ^oC for 1min. Develop the PR in MF -319(Microposit) for 40-50 s. Rinse and dry the wafer and then hard bake it at 115 ^oC for 2 min. Prepare ITO etchant of 8-9:1:15 (HCL:HNO_3:H_2O) and etch the exposed ITO at 50 ^oC for 3-4 min. Rinse and dry the wafer, check the features then dice wafer in to individual chips. After dicing strip off the PR on the chips using Baker Aleg -355 stripper at 40 ^oC for 2 min. After stripping, rinse and dry the wafer then dehydrate at 150 ^oC for 10min. [20], [21]

After forming electrodes on chips, chips were coated with 1μm of SiO_2 using PECVD for a dielectric layer. After completion of PECVD contact pads are covered with tape and spin coated with PR, then tape is removed, then the substrates were soft-baked on hot plate (115C, 1 min) and then dipped in SiO_2 etchant (2 min). Finally the PR was stripped using stripper, and then the substrates were dehydrated. SU-8 5 can also be used as dielectric layer instead of SiO_2. In the process for SU-8 5 deposition first keep the chips in buffer oxide etchant for 10 min

then clean and dehydrate the chips at 150 ^{o}C for 10min. Cover the contact pads with tape then spin coat SU-8 5 at 3000 rpm for 30 s (ramp rate 300 rpm/s) to form a uniform thickness of 5 μm then remove the tape and soft-bake at 65 ^{o}C for 1min then at 95 ^{o}C for 3min. Expose the SU-8 5coated wafer to UV light using OAI Aligner (I-Line 365 nm) to an expose dosage of 140 mJ/cm^2 for 6.5 s then bake at 65 ^{o}C for 1 min then at 95 ^{o}C for 1 min and then hard bake by ramping up to 175 ^{o}C for 8 min. Teflon solution was prepared by dissolving 2 % (w/v) of Teflon AF1600 (www2.dupont.com, Wilmington, DE) in Fluoroinert FC75 solvent (www.fishers-ci.com, Barrington, IL). Spin coat the patterned ITO chip and un-patterned ITO cover slide with Teflon – AF at 1000 rpm for 30 s to form a layer of 200 nm thickness then for Teflon treatment bake the chips and cover slides at 115 ^{o}C for 10 min then, ramp up to 165 ^{o}C, bake at 165 ^{o}C for 10 min and then, ramp up to 330 ^{o}C, bake at 330 ^{o}C for 20 min which forms a hydrophobic layer. [20], [21]

2.2.3. Setup

Each device was assembled with an un-patterned ITO coated glass substrate on the top which forms a contiguous electrode and a patterned substrate at the bottom separated by a spacer formed from one piece of double sided tape (~100 μm thick) as shown in figure 2.10 Cross sectional view of EWOD setup. Droplets are sandwiched between the plates and are actuated by applying electric potential between the top electrode and sequential electrode on the bottom plate. The top cover slide acts as the ground and voltages are applied on bottom electrode electrodes. A potential (80-100 V_{RMS}) is applied between the electrodes. The chip is inserted in to the PCI slot and the PCI is connected to the DAQ system through switches with ribbon cables. Individual switches can be actuated with Labview software which is interfaced with DAQ system. Thus the actuation of the electrodes can be controlled through labview programming.

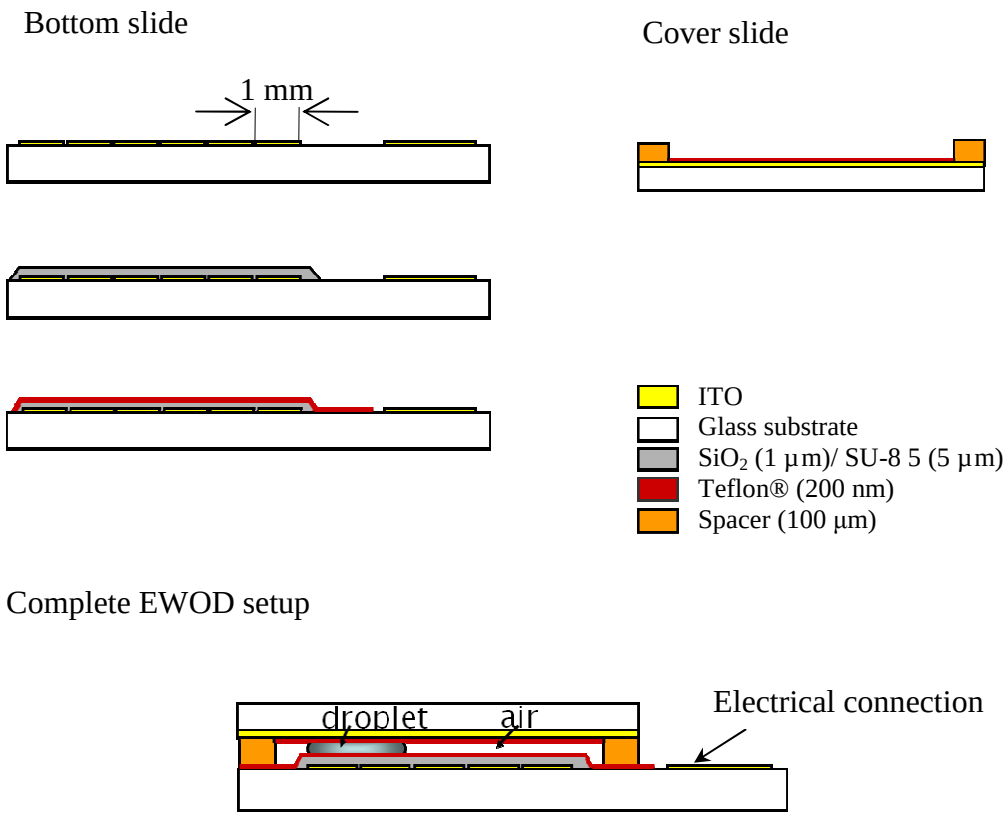

Figure 2.10 Cross sectional view of EWOD setup.

2.3 Control of EWOD Device

Control board for EWOD actuation was made to actuate all the actuation electrodes individually with Labview interface. The off-chip control circuit used to drive droplets on the patterned electrodes consists of a series of semiconductor relay (NAiS AQW614EH) and resistors (1 kΩ) coupled in a manner (figure 2.11 and figure 2.12) to selectively turn on or off.

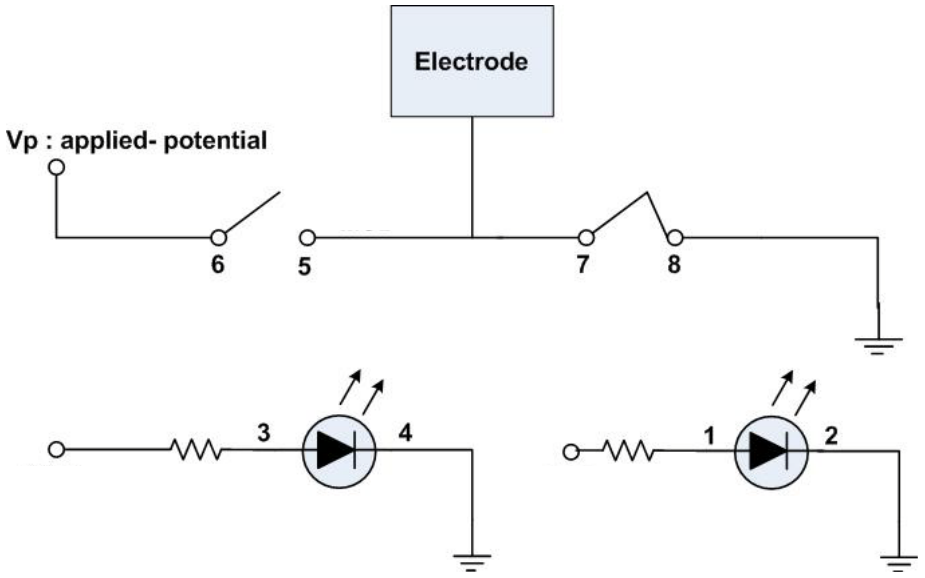

Figure 2.11 Relay configuration (NAiS AQW614 EH) ,5 - 6: Normally Open (NO),
7 – 8: Normally closed (NC)

National Instruments Data Acquisition board NI USB-6609 with connector NI SCB 100 was used. DAQ PAD 6507 is a 96-bit digital I/O interface for computers with USB ports. A relay contacts are enabled only when it received a “hi or 1V” from Digital I/O.

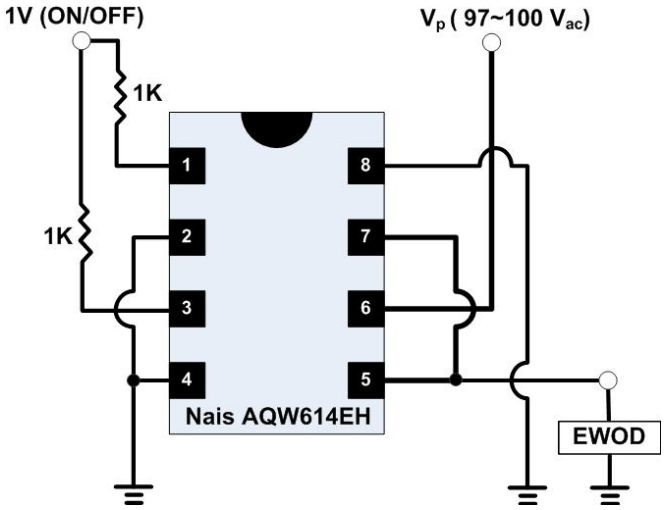

Figure 2.12 Control Circuit design

The program for Individual Electrode actuation of EWOD chip was made in Labview. When we run the program, it opens a front panel window (figure 2.13), and the block diagram (figure 2.14).

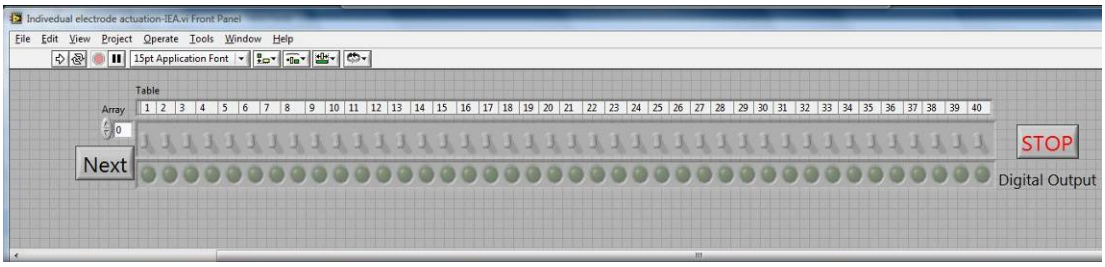

Figure 2.13 Individual Electrode actuation program Front panel view.

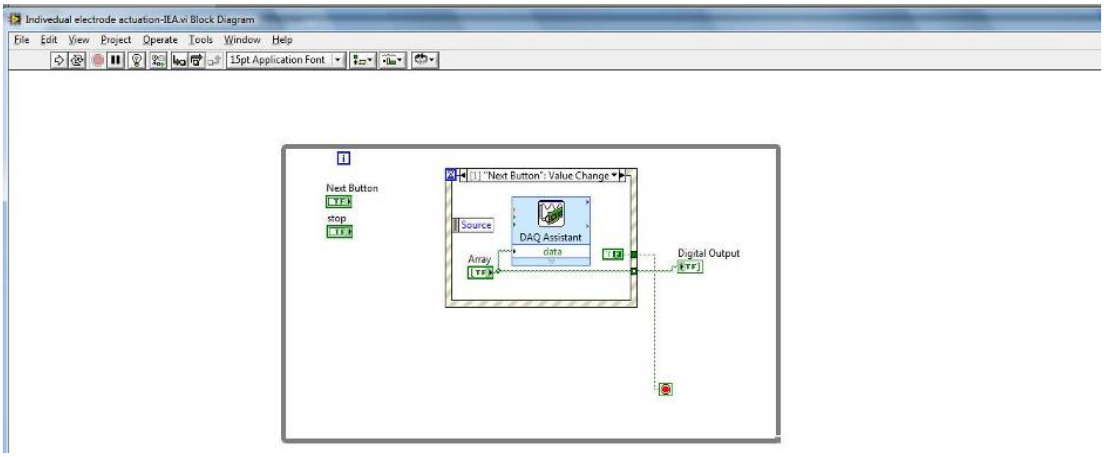

Figure 2.14 Individual Electrode actuation program Block diagram view.

When you run the program switch on the required electrode and click Next button. In the next step switch off the unnecessary electrode and turn on required electrodes in step 2 and click next button and so on. One of the intermediate steps is shown in figure 2.15.

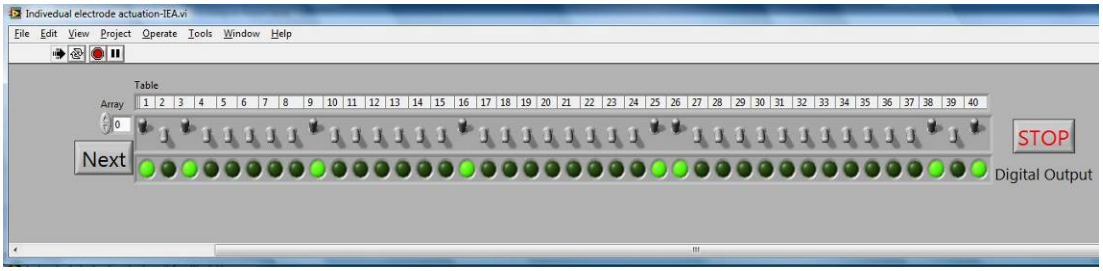

Figure 2.15 Intermediate step in Individual Electrode actuation program.

Another Labview program was created which is an automated program, considering a predefined flow path of the droplet. The program allows modification of the droplet handling and extraction time, and can define the path of the droplet. The front panel and block diagram of the program is as shown in figure 2.16 and figure 2.17.

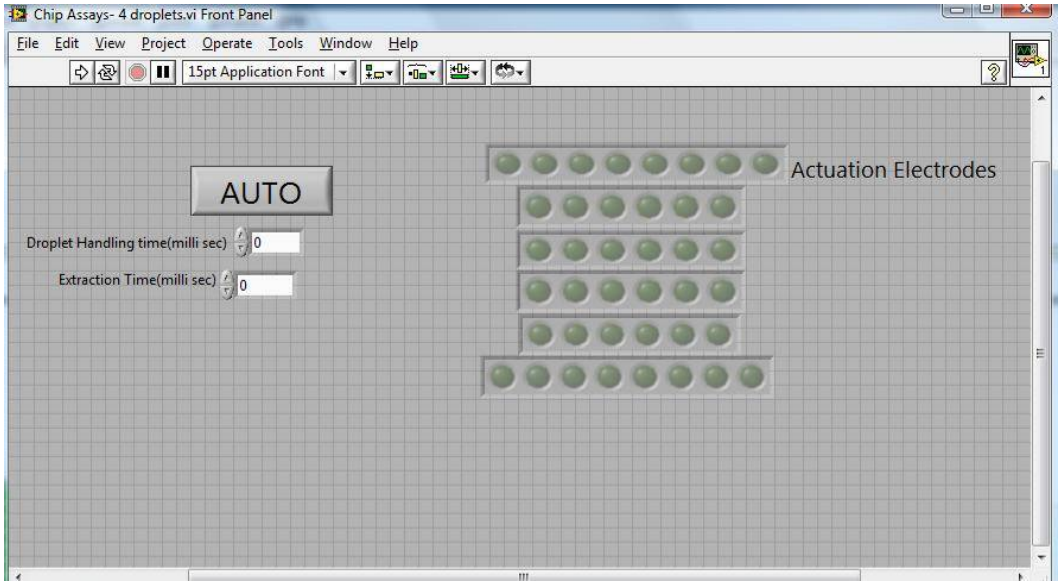

Figure 2.16 Auto 4 droplets generation program front panel view.

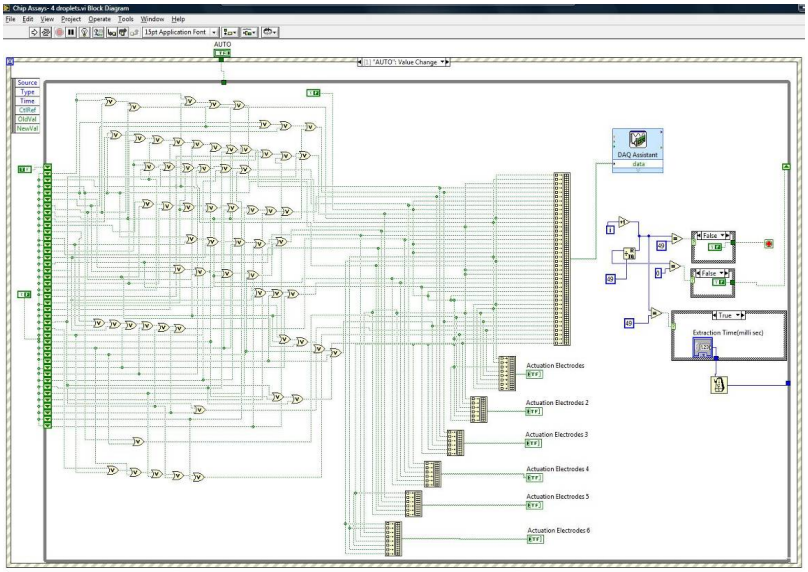

Figure 2.17 Auto 4 droplets generation program Block diagram view.

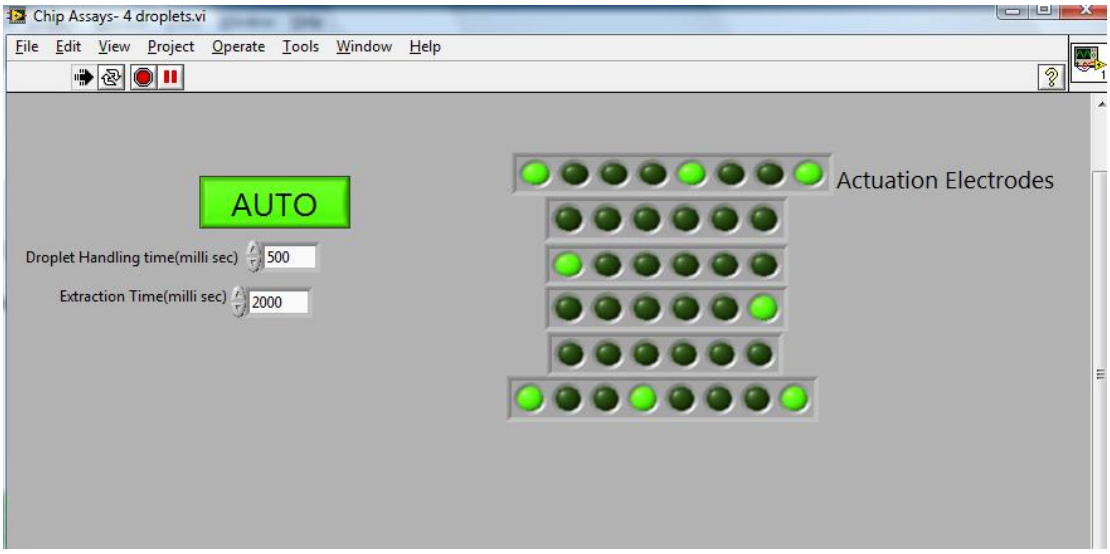

Figure 2.18 Intermediate step in Auto 4 droplets generation program.

Figure 2.18 shows an intermediate step in the program where the droplet handling time is 500 ms and the extraction time is 2000 ms. If more than one extraction or mixing sequence is necessary, we can include that particular step in the program, that results in common extraction time. If different time spans are necessary, adding another loop in the program will provide different time span for extraction and mixing.

2.4 Spectrophotometry measurement

When the concentration of the solute is very low, it is very difficult to visually conclude the success of the extraction. In order to quantify the extraction we built a small spectrophotometry setup as shown in figure 2.19. The setup consists of a platform where we can place the EWOD chip. An LED of designated wavelength was used to pass the light which was streamlined by an optical fiber to pass through the EWOD chip, where a high sensitive light intensity to voltage converter (TSL257-TAOS) was arranged on the other side to give the reading of voltage corresponding to the intensity of light passing through the EWOD chip. Comparing the difference in the voltages recorded, we can quantify the extraction.

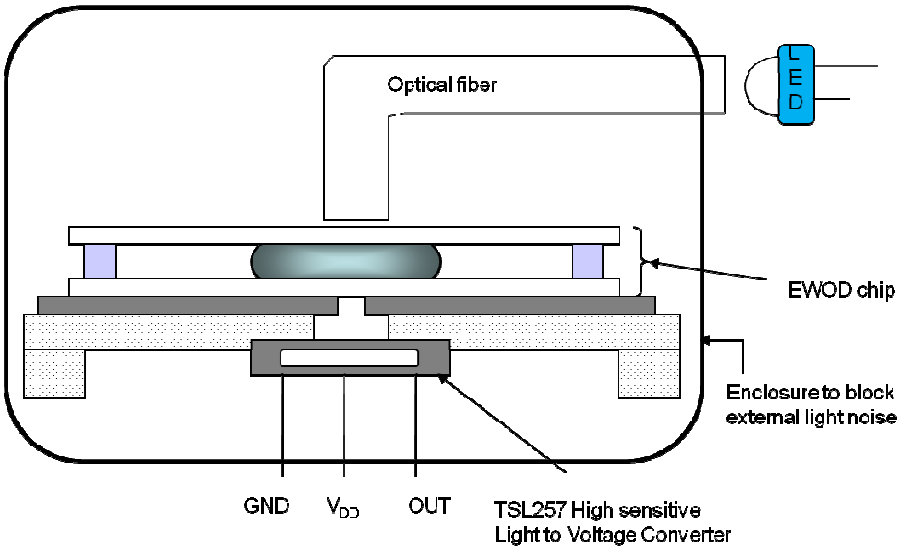

Figure 2.19 Spectrophotometry setup for EWOD.

CHAPTER 3

RESULTS

3.1 On-chip liquid-liquid microextraction and separation

3.1.1. Basic procedure for on chip microextraction and separation

Liquid-liquid extraction is the transfer of certain components (e.g. solutes) from one phase to another when immiscible or partially soluble liquid phases are brought into contact with each other. Solutes including nucleic acids and proteins of interests can be extracted from one liquid phase to the other immiscible liquid phase as a preparation step for many analytical processes. There are several advantages in miniaturizing the liquid-liquid extraction methods to on-chip level extraction. Usual advantages of miniaturization are the reduction in the sample size and portability. In addition, transport phenomena is faster in micro-systems than in ordinary size systems, and therefore, one may expect that liquid-liquid extraction takes less time to achieve in miniaturized devices. It is due to shorter diffusion time in micro scale as well as high surface to volume ratio of microsystems. However, in microchannel, due to its very low Reynolds number, two immiscible liquid phases contact each other with limited interfacial area where extraction process takes place. Thus, performance enhancement of the purification or isolation by liquid-liquid extraction by using microchannel flow is hindered despite its small scale. Interface can be increased by segmenting (or digitizing) a continuous liquid flow into droplet based flow.

Electrowetting on dielectric (EWOD) digital microfluidics is an efficient platform to process droplet based analytical processes. Nanoliter (nL) or smaller volume of aqueous liquid droplets can be generated and transported on a chip by EWOD process. We selected DI water as one phase and room temperature ionic liquid (RTIL) as a second liquid phase for extraction, which forms immiscible interface with each other. The generation of droplet from the reservoir is

generally carried by actuating the adjacent actuation electrodes and then, actuating both reservoir and the particular electrode creates necking and generates the droplet from the reservoir as shown in figure 3.1 (a). After generation of the two droplets (one from liquid A and the other from liquid B with solute), they were brought together for the extraction by actuating the required electrode as shown in figure 3.2 (b).

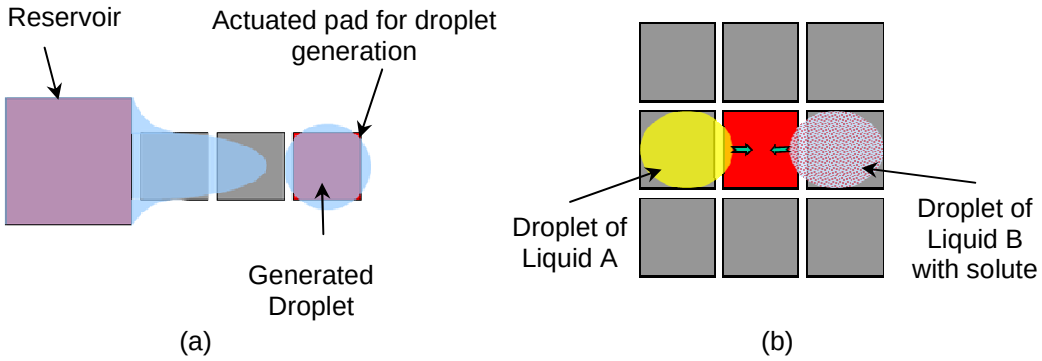

Figure 3.1 Generation and mixing of two liquid phases on-chip (a) generation (b) mixing

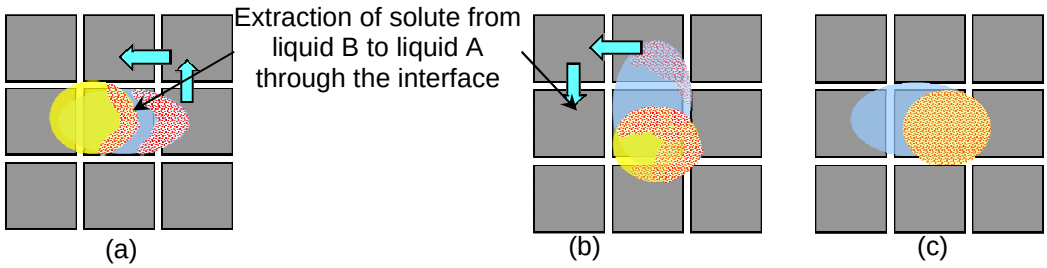

Figure 3.2 Microextraction process

When the two liquid phases join together an interface is formed where the solute particles from liquid B extracts to liquid A. New interface was provided between the two droplets to enhance the extraction by moving one liquid droplet around the other to avoid the saturation or equilibrium at the interface as shown in figure 3.2. High chemical potential can be maintained at the interface in droplet based extraction when the droplets are in motion

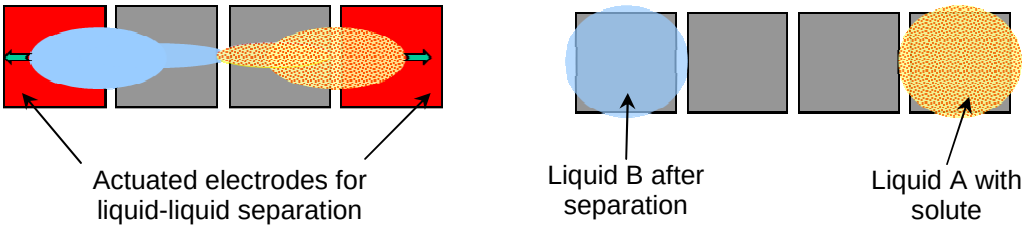

Figure 3.3 Separation process

After the interface enhanced extraction, the important part is separating the two liquid phases at the microscale. Separation of the two liquid phases is very important because, in protein purification we have to perform multiple steps of extraction on chip. In order to perform multiple extractions we should be able to separate the two liquid phases after each extraction. Extraction of the two liquid phase droplets on chip is carried by actuating the electrodes in such a way that, two droplets pull away from each other forming a neck in between at first and then separation proceeds as shown in figure 3.3.

3.1.2. Ionic Liquids

Ionic liquids (IL) are environmentally friendly alternatives to organic solvents for liquid-liquid extraction. They reduce the related costs, disposal requirements, and hazards associated with volatile organic compounds. Room Temperature Ionic Liquids (RTIL) are salts that are liquids over a wide temperature range, including room temperature. The ability to fine-tune the properties of the ILs will allow selection of IL to replace specific solvents making them “task-specific” ionic liquids (TSIL). [22]-[24]

ILs importance comes from its properties of high ionic conductivity, non-volatility, non-flammability, high thermal stability. The important characteristic of RTIL is that it can be tailored by choice of cation, anion and substituent’s. They have a wide range of applications in catalysis, synthesis, electrochemistry, and separations. Although it promises high performance biomolecules extraction, finding TSIL is still very challenging because the process utterly relies

on “trial-error” method. Thus, high-throughput screening (HTS) devices are desired to facilitate discovery of TSILs for biomarkers. [25]-[30]

3.1.3. Extraction of dye and separation

Liquid-liquid extraction was performed by sandwiching the DI water and 1-butyl-3-methylimidazolium bis(trifluoromethylsulfonyl)imide, [bmim][NTf_2] with dye suspended in it at the reservoirs shown in figure 3.4 (a). Dye suspended [bmim][NTf2] and DI water droplets were successfully generated from their respective reservoirs by EWOD operation as shown in figure 3.4 (b)-(e). Generated droplets were brought together by EWOD operation, which created an interface between the two liquid phases as DI water is immiscible with [bmim][NTf2] shown in figure 3.4 (f). As soon as the dye at interface region comes in contact with DI water, it diffused from [bmim][NTf2] to DI water as shown in figure 3.5 (a). The interface between the two liquid phases is increased to enhance the extraction by surrounding the DI water with dye suspended [bmim][NTf2] as shown in figure 3.5 (b), (c). After the extraction [bmim][NTf2] was separated from dyed DI water by actuating the specific electrodes using EWOD operation.

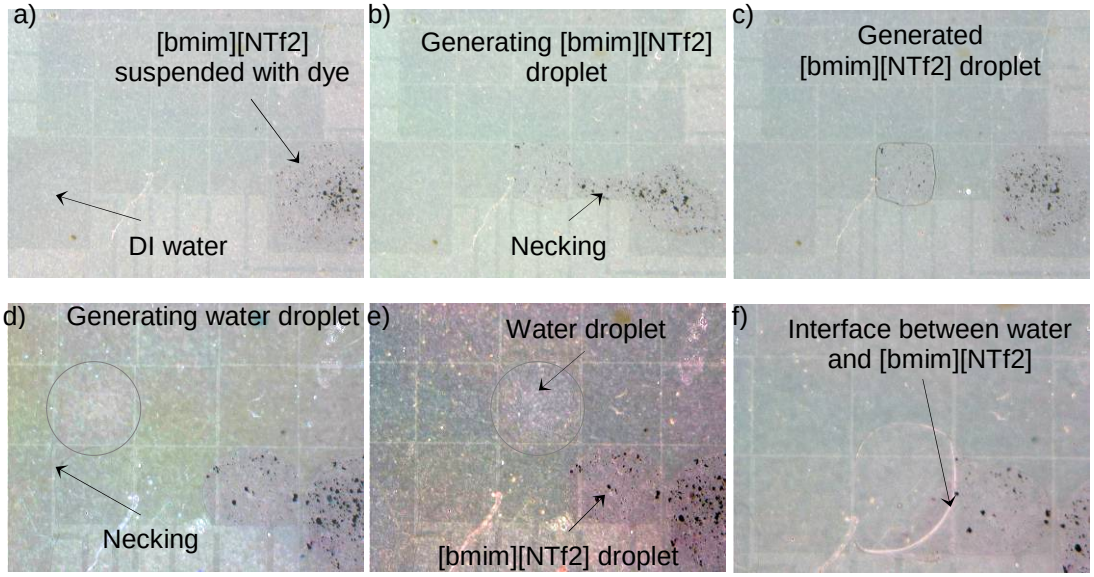

Figure 3.4 Sequential images at different stages of micro extraction of dye process (images are captured from video recording experiment). (a) - (e) Dispensing of dye suspended [bmim][NTf2] droplet and DI water from their reservoir drop. (f) Shows the merging of DI water droplet with IL.

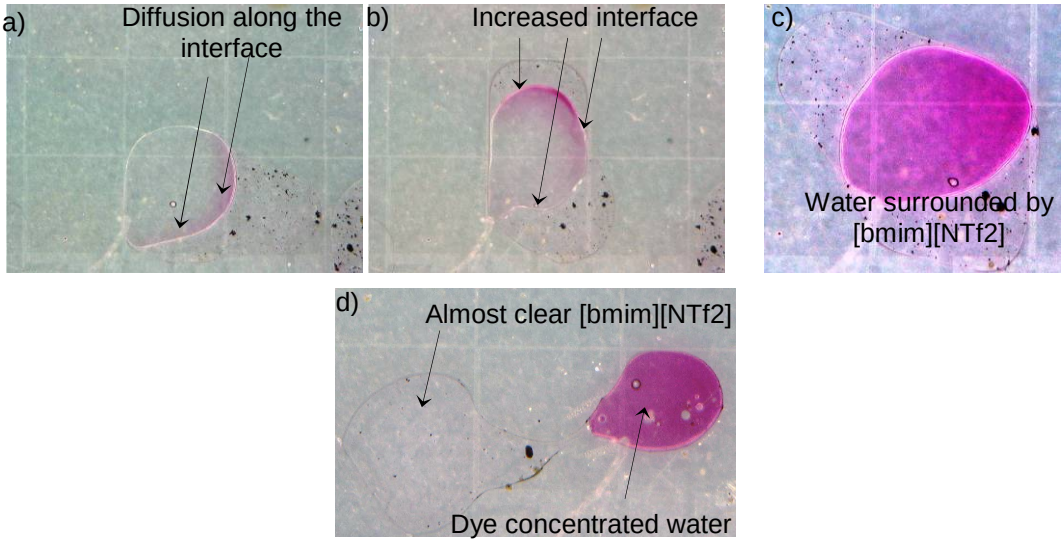

Figure 3.5 Sequential images at different stages of micro extraction of dye process continuation. (a) Diffusion of dye from RTIL to water. (b) & c) Increased interface between water and RTIL by surrounding the water with RTIL. (d) Separation of the RTIL and dye concentrated water.

3.1.4. Extraction of Iodine (I_2), separation and detection

Liquid-liquid extraction was performed by sandwiching the Iodine dissolved DI water and [bmim][NTf2] at the reservoirs shown in figure 3.6(a). A [bmim][NTf2] droplet was successfully generated from a large reservoir drop by using EWOD operation, then transported to the extraction site and joined with a droplet of second liquid phase which is iodine rich DI water as shown in figure 3.6 (c) and (d). As soon as two immiscible liquid phases joined together, an interface formed in between as shown in figure 3.6 (d). Then iodine molecules started diffusing into [bmim][NTf2] to decrease the chemical potential at the interface and achieve the equilibrium (figure 3.6 (d)). As iodine extraction progressed further, the color of [bmim][NTf2] droplet became more yellowish while water phase decolorized and becomes clear water droplet as shown in figure 3.6 (e). After successful extraction, iodine rich [bmim][NTf2] droplet was separated from the water phase using EWOD operation resulting in complete selective separation of iodine from aqueous solution sample. The separation process is demonstrated in figure 3.6 (f). The complete separation was successfully demonstrated,

however, iodine concentration within [bmim][NTf2] solution was not uniformly distributed due to its high viscosity (figure 3.7 (a)). By translating the [bmim][NTf2] droplet with unevenly distributed iodine by EWOD operation, we could stimulate further diffusion of iodine within the droplet and achieve more even distribution of iodine molecules as shown in figure 3.7 (b). Figure 3.7 (c) demonstrates the iodine extraction into [bmim][NTf2] by comparing its color with that of a pure [bmim][NTf2] droplet.

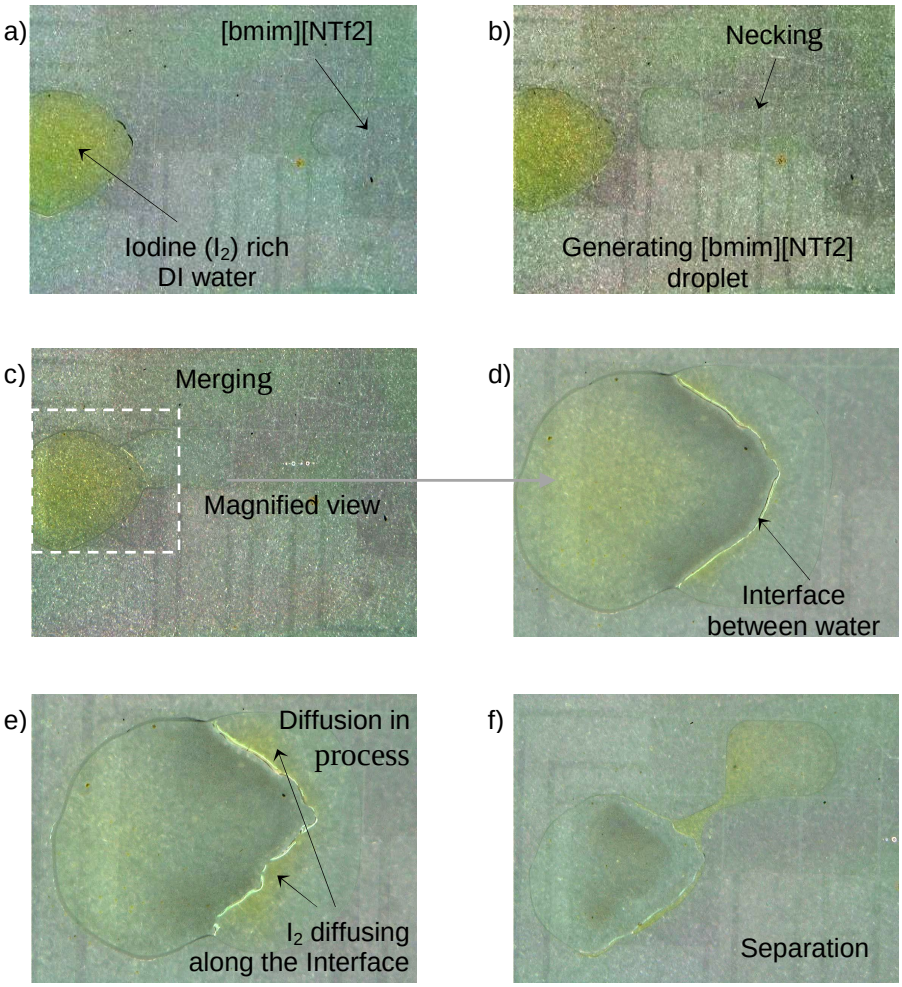

Figure 3.6 Sequential images at different stages of micro extraction of Iodine process (images are captured from video recorded experiment). (a) – (c) Dispensing of RTIL droplet from reservoir drop and its merging with I_2 rich DI water droplet. (d) Enlarged image at the interface. (e) Diffusion of I_2 from water to RTIL. (f) Separation of I_2 rich RTIL droplet.

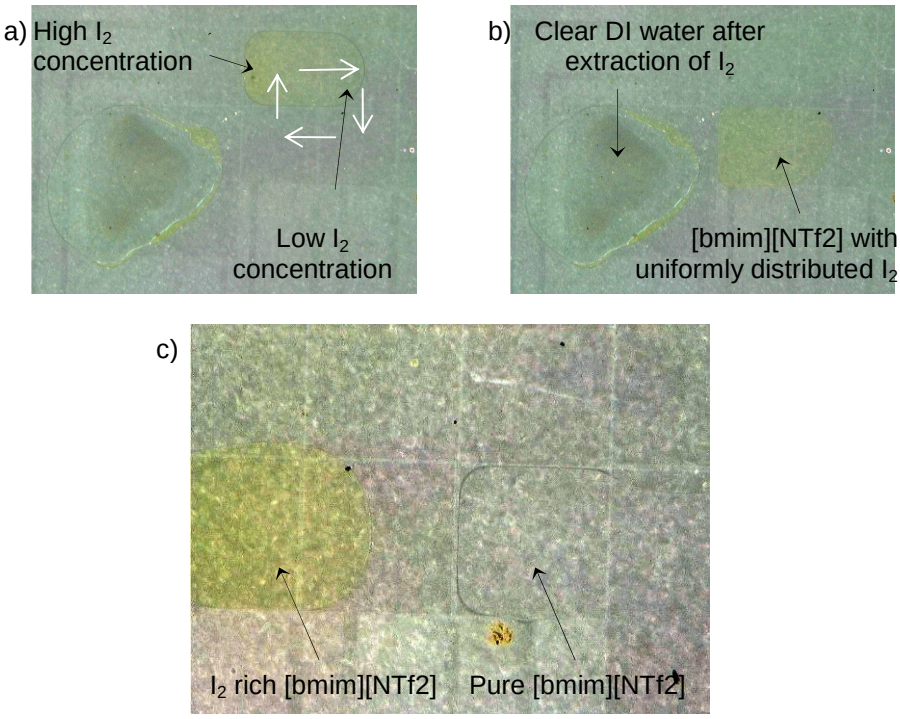

Figure 3.7 Sequential images at different stages of micro extraction of Iodine process continuation. (a) After separation, part of RTIL has higher concentration of I_2. Droplet motion with direction indicated with white arrows stimulated diffusion of I_2 within RTIL droplet. (c) Uniform distribution of I_2 in RTIL after forced diffusion.

To quantify the extraction concentration, spectrophotometry (described in section 2.4) setup was used. For Iodine extraction experiment, an LED of 555nm wavelength was used, because of Iodine color. Voltage detected by the sensor for EWOD setup without any liquid medium (air), voltage detected with [bmim][NTf2] and voltage detected with I_2 extracted [bmim][NTf2] were tabulated in table 3.1. Voltage comparisons show the lower voltage for higher concentration of Iodine extracted [bmim][NTf2].

Table 3.1 Spectrophotometry voltage measurement of I_2 extraction

	Voltages detected when Iodine is extracted from DI water to [bmim][NTf2]		
	Air (volts)	*Pure [bmim][NTf2] (volts)*	*I_2 extracted [bmim][NTf2] (volts)*
Voltage	4.04	3.75	3.0~3.48

3.2 On chip pH dependent partitioning in RTILs

RTIls compatibility in solvent extraction was demonstrated by Ann E. Visser et.al. [31]. It considered the reversible pH dependent liquid-liquid partitioning which was demonstrated by using the indicator dye, thymol blue. Investigations incorporate that the partitioning of thymol blue as a function of aqueous phase for a series of 1-alkyl-3-methylimidazolium hexafluorophosphates ([Cnmim][PF6]). [31]

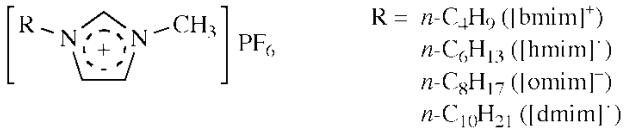

Figure 3.8 Structural variations in the 1-alkyl-3-methylimidazoliumhexafluorophosphate salts used in this study. [31]

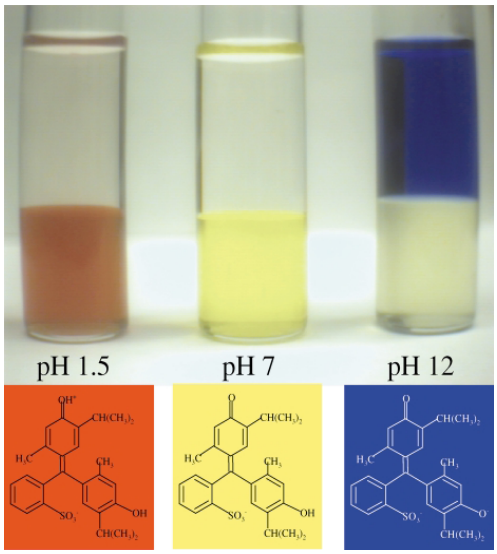

Figure 3.9 The phase preference of the three forms of thymol blue in [bmim][PF6]. [31]

Figure 3.9 illustrates the qualitative partitioning of thymol blue in its three forms between aqueous (top) and 1-butyl-3-methyl-imidazoline hexafluorophosphate [bmim][PF6] (bottom) phases as aqueous phase pH is changed from very acidic (<2) to very basic (>10). At low pH thymol blue exists in its red form as a neutral zwitterion which prefers the RTIL phase

[32]-[34]. As the pH is increased by addition of NaOH, the yellow monoanion forms with some detect ability increase in concentration in the aqueous phase. The blue dianion, above pH = 10, partitions quantitatively to the aqueous phase. [31]

On chip pH dependent partitioning in RTILs using EWOD was demonstrated by considering [bmim][PF6] and thymol blue in acidic medium which was prepared off chip in the proportions of 5 µl acetic acid (5%), 12 µl DI water, 8 µl saturated thymol blue solution. The reason for diluting the acetic acid was that at micro level acetic acid was not immiscible with [bmim][PF6]. Liquid-Liquid extraction of thymol blue was performed by sandwiching the [bmim][PF6] solution and acidic solution with thymol blue which was describe earlier, at the reservoirs. Thymol blue sample and [bmim][PF6] droplets were successfully generated from large reservoir drops by EWOD operation, then transported for extraction as shown in figure 3.10 (a) – (g). When the two droplets were brought together by EWOD operation, an interface was formed between them as shown in figure 3.10 (h). As the thymol blue prefers RTIL when it is in acidic medium interface, thymol blue was extracted in to [bmim][PF6] droplet which is shown in figure 3.11 (a) - (b). After the extraction the two liquid phases were separated by selective operation of electrodes as shown in figure 3.11 (c).

Extraction concentration was quantified by Spectrophotometry method (described in section 2.4). For thymol blue extraction experiment, an LED of 620nm wavelength was used. Voltage detected by the sensor for EWOD setup without any liquid medium (air), voltage detected with [bmim][PF6] and voltage detected with thymol blue extracted [bmim][PF6] were tabulated in table 3.2. Voltage comparisons show the lower voltage for the increase in concentration of thymol blue extracted [bmim][PF6].

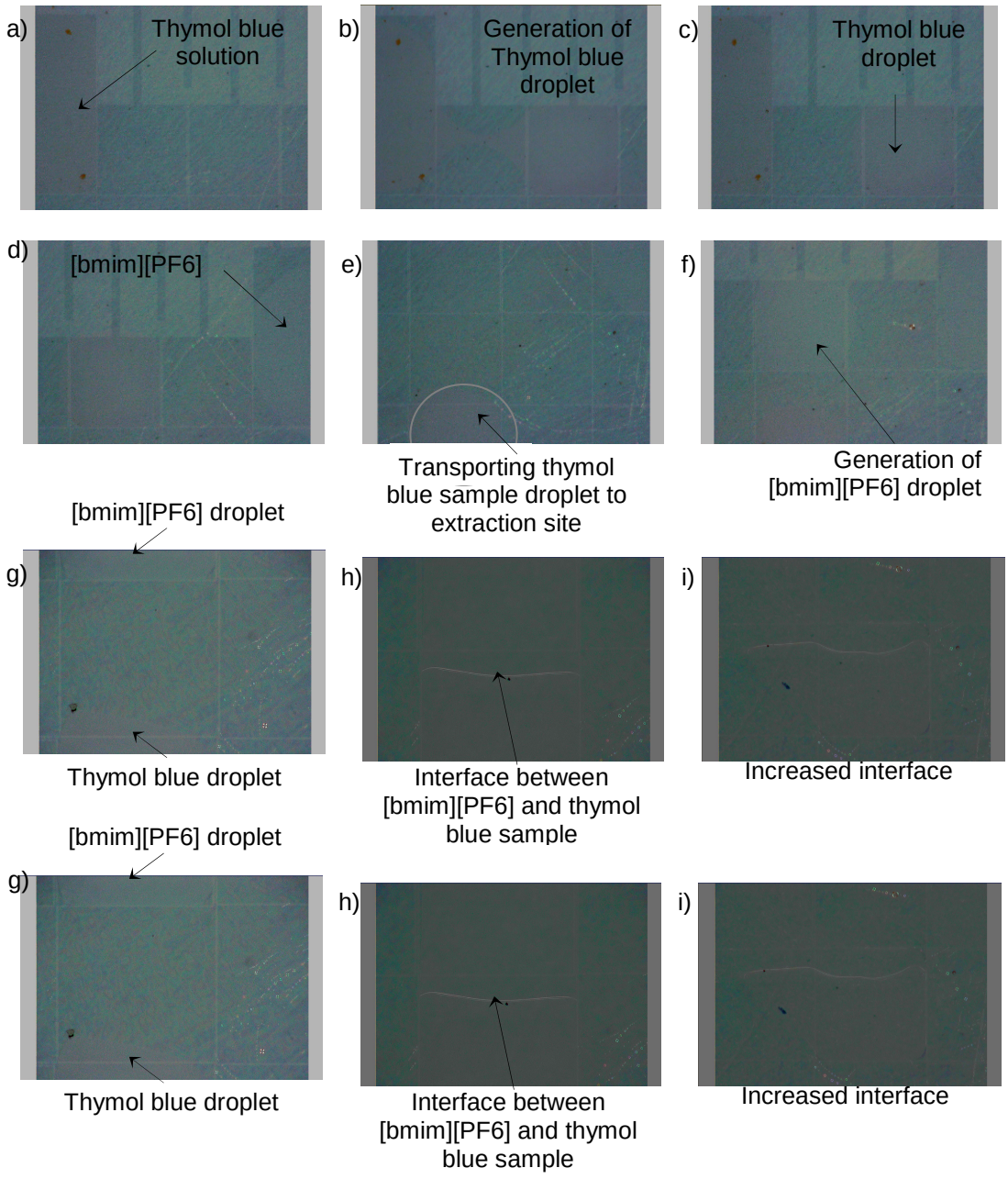

Figure 3.10 Sequential images at different stages of micro extraction process (images are captured from video recording experiment). (a) - (f) Dispensing of thymol blue acidic sample droplet and [bmim][PF6] from their reservoir drop. (h) Shows the merging of thymol blue sample droplet with [bmim][PF6] droplet.

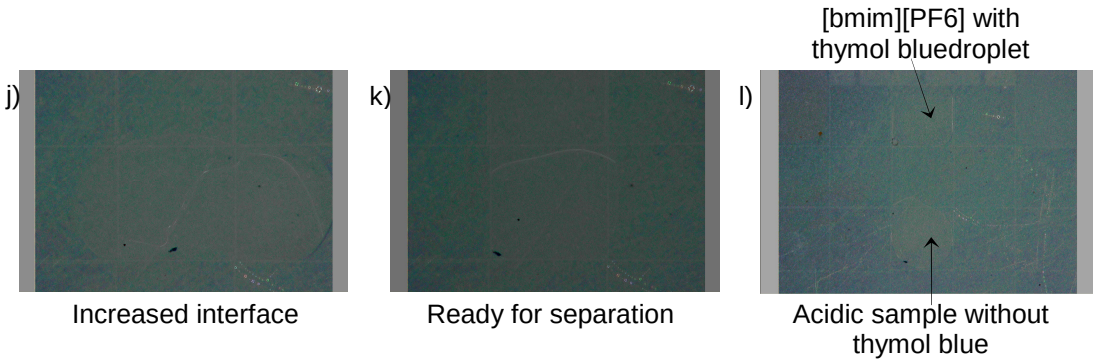

Figure 3.11 Sequential images at different stages of micro extraction process continuation. (a) - (b) Increased interface between thymol blue sample and RTIL. (c) Separation of [bmim][PF6] with thymol blue and Acidic sample.

Table 3.2 Spectrophotometry voltage measurement of thymol blue extraction

Voltage measurement of absorbance optical detection	Voltage detected when thymol blue is extracted from acidic aqueous solution to [bmim][PF6]		
	Air (volts)	*Pure* [bmim][PF6] *(volts)*	thymol blue extracted [bmim][PF6] *(volts)*
Voltage	1.48	1.43	1.31~1.35

An on chip pH dependent partitioning in RTIL's using EWOD operation was performed to demonstrate that, pH value of the aqueous solution effect the extraction process. On-chip pH dependent partitioning in RTIL's experiment demonstrates that on chip pH titration and on chip pH dependent extraction is possible which can lead to on chip synthesis of RTIL's and HTS.

CHAPTER 4

CONCLUSION AND FUTURE WORK

4.1 Conclusion

Successful on-chip microextraction was demonstrated using EWOD digital microfluidic platform with two model experiments. One was extraction of organic dye from RTIL ([bmim][NTf2]) to DI water. Second one was extraction of iodine (I_2) from water to [bmim][NTf2]. Use of RTIL on EWOD platform and successful basic digital fluidic functions (e.g. transporting, generating, joining, and separating) have been achieved and reported for the first time. On chip pH dependent partitioning in RTIL's using EWOD operation was demonstrated by extracting thymol blue from Acidic medium to [bmim][PF6], which can lead to high-throughput screening (HTS) synthesis of RTIL's and HTS of protein extraction.

Complete selective separation of solute from a sample phase to counter phase has been demonstrated. This demonstration is the first step toward a micro total analysis system (μTAS). The presented result opens the way to on-chip micro extraction, which will be readily integrated with other sample preparation microfluidic components and detection components.

4.2 Future work

High-throughput screening (HTS) for protein extraction using "task-specific" ionic liquid (TSIL) can be achieved in near future. Integration of synthesis module, extraction module and data interpretation module on to a single chip will lead to μTAS which is currently in progress.

REFERENCES

1. Frank M Wite, Fluid Mechanics: Tata McGraw-Hill; 2008.

2. KE.Herold, A.Rasooly,Lab-on-a-Chip Technology: Fabrication and Microfluidics: Caister Academic Press, 2009.

3. KE.Herold, A.Rasooly,Lab-on-a-Chip Technology: Biomolecular Separation and Analysis: Caister Academic Press, 2009.

4. Nano Fusion Technologies, Inc. http://www.nft-eop.co.jp/en/technology/multilaminarflow .html

5. B.Bustgens, W.Bacher, W.manz and W.K.Schomburg, "Micropump manufactured by thermoplastic molding", *Proc. Micro Electro Mech. Sys.'94*, 18-21, 1994.

6. H.Helvajian, Microengineering aerospace systems: AIAA; 1999.

7. Nano fusion Technologies www.nft-eop.co.jp/en/technology/droplet.html

8. Y.H.Chang, G.B.Lee, F.C.Huang, Y.Y.Chen and J.L.Lin, "Integrated polymerase chain reaction chips utilizing digital microfluidics," *Biomed Microdevices*, pp.8(3) 215-25,2006.

9. Jessica Melin, Stephen R. Quake., "Microfluidic Large-Scale Integration: The Evolution of Design Rules for Biological Automation," *Annual Review of Biophysics and Biomolecular Structure*, Vol. 36, pp. 213-231, 2007.

10. M.G.Lippmann, *Ann. Chim. Phys.*, Vol. 5, pp.494, 1875.

11. F.Saeki, J.Baum, H.Moon, J.Yoon, C.J.Kim and R.Garrell, *Polym. Mater. Sci. Eng*., Vol. 12, pp. 85, 2001.

12. S.K.Cho, S.K.Fan, H.Moon and C.J.Kim, "Towards digital microfluidic circuits: creating, transporting, cutting and merging liquid droplets by electrowetting-based actuation ," *IEEE Micro Electro Mechanical Systems Workshop*, Las Vegas, NV, pp.32, 2002.

13. S.K.Cho, H.Moon, J.Fowler and C.J. Kim, *Proceeding of ASME IMECE*, New York, NY, MEMS-23831, 2001.

14. W. Adamson, Physical Chemistry of Surfaces, New York: J Wiley; 1990.

15. R.R.Tummala, Fundamentals of microsystems packaging: McGraw-Hill Professional; 2001.

16. M.J.Madou, Fundamentals of microfabrication: CRC Press, 2002.

17. UTA Nano fabrication facility http://www.uta.edu/engineering/nano/facilities.php

18. Mems and nanotechnology exchange
http://www.memsnet.org/mems/processes/deposition.html

19. I.Barbulovic-nad, H.Yang, P.S. park, A.R.Wheeler, "Digital microfluidics for cell-based assays," *The Royal Society of Chemistry, Lab Chip*, pp.519–526, 2008.

20. H.Moon, S.K.cho, "Low voltage electrowetting-on-dielectric," *Journal of Applied Physics*, Vol.92(7), pp.4080-4088, 2002.

21. H.Moon, A.wheeler, R.L.Garrell, J.A.Loo, C.J.Kim, "An Integrated Digital Microfluidic Chip for Multiplexed Proteomic Sample Preparation and Analysis by MALDI-MS", *Lab Chip* , Vol.6, pp.1213-1219, 2006.

22. K.R. Seddon, “Ionic Liquids for clean Technology,” *Journal of Chemical Technology & Biotechnology*, Vol. 68(4), 1999.

23. C.J.Bowlas, D.W.bruce, and K.R.Seddon, “Liquid-crystalline ionic Liquids,” *Chemical Communications*, issue 16, pp. 1625,1996.

24. .S.Wilkie and M.J.Zaworofko, “Air and water stable 1-Ethyl-3-methylimidazolim based IL’s,” *Chemical Communications*, issue 8, pp. 965, 1992.

25. J.G.Huddleston, H.D.Willauer, R.P.Swatloski, A.E.Visser and R.D.Rogers,"Room temperature ionic liquids as novel media for clean liquid–liquid extraction," *Chemical Communications*, issue 16, pp.1765, 1998.

26. M.J.Earle, K.R.Seddon, C.J.Adams and G.Roberts, "Friedel–Crafts reactions in room temperature ionic liquids," *Chemical Communications*, issue 19, pp.2097, 1998.

27. P.J.Dyson, D.J.Ellis, D.G.Parker and T.Welton, "Arene hydrogenation in a room-temperature ionic liquid using a ruthenium cluster catalyst," *Chemical Communications*, issue 1, pp.25, 1999.

28. M.J.Earle, P.B.McCormac and K.R.Seddon, "Regioselective alkylation in ionic liquids," *Chemical Communications*, issue 20, pp.2245, 1998.

29. M.J.Earle, P.B.McCormac and K.R.Seddon,"Diels–Alder reactions in ionic liquids . A safe recyclable alternative to lithium perchlorate–diethyl ether mixtures," *Green Chemistry*, issue 1, pp.23, 1999. 24.

30. T.Welton, "Room-Temperature Ionic Liquids. Solvents for Synthesis and Catalysis," *Chemical Reviews*, Volume 99, Issue 8, 1999.

31. Ann E. Visser, Richard P. Swatloski and Robin D. Rogers "pH-Dependent partitioning in room temperature ionic liquids provides a link to traditional solvent extraction behavior," *Green Chemistry*, pp.1, 2000.

32. C.M.Gordon, J.D.Holbrey, A.R.Kennedy and K.R.Seddon, "Ionic liquid crystals: hexafluorophosphate salts," *Journal of Materials Chemistry*, Vol.8(12), pp.2627, 1998.

33. J.D.Holbrey and K.R.Seddon, "The phase behaviour of 1-alkyl-3-methylimidazolium tetrafluoroborates; ionic liquids and ionic liquid crystals," *Journal of the Chemical Society, Dalton Transactions*, issue 13, pp.2133, 1999.

34. G.F.Nalven and S.M.Smith, Lange's Handbook of Chemistry, New York: McGraw-Hill; 1992.

BIOGRAPHICAL INFORMATION

Praveen Kunchala did his B.Tech at Nagarjuna university, Guntur, INDIA, currently persuing M.S in Mechanical engineering. He is currently working in IMNF lab (Dr. Hyejin Moon). His areas of interests are microfabrication, microfluidics, Bio-MEMS, EWOD.